

# **The Extreme Positive Indian Ocean Dipole of 2019 and Associated Indian Summer Monsoon Rainfall Response**

**Satyaban B. Ratna<sup>1</sup>, Annalisa Cherchi<sup>2</sup>, Timothy J. Osborn<sup>1</sup>, Manoj Joshi<sup>1</sup> and Umakanth Uppara<sup>1</sup>**

Formatted: English (US)

<sup>1</sup>Climatic Research Unit, School of Environmental Sciences, University of East Anglia, Norwich, NR4 7TJ, United Kingdom

<sup>2</sup>Institute of Atmospheric Sciences and Climate (ISAC-CNR), Bologna, Italy

Corresponding author: Satyaban B. Ratna (S.Bishoyi-Ratna@uea.ac.uk)

## **Key Points:**

- The positive Indian Ocean Dipole event that occurred in 2019 was among the strongest in the modern instrumental record
- The 2019 Indian Summer monsoon exhibited an unusual seasonal evolution with dry conditions in June but resulted in above normal rainfall
- The seasonal evolution of ISM was partly driven by a combination of equatorial Pacific and Indian Ocean sea surface temperature anomalies

24 **Abstract**

25 The positive Indian Ocean Dipole (IOD) event in 2019 was among the strongest on record,  
26 while the Indian Summer monsoon (ISM) was anomalously dry in June then very wet by  
27 September. We investigated the relationships between the IOD, Pacific sea surface temperature  
28 (SST) and ISM rainfall during 2019 with an atmospheric general circulation model forced by  
29 observed SST anomalies. The results show that the extremely positive IOD was conducive to  
30 a wetter-than-normal ISM, especially late in the season when the IOD strengthened and was  
31 associated with anomalous low-level divergence over the eastern equatorial Indian Ocean and  
32 convergence over India. However, a warm SST anomaly in the central equatorial Pacific  
33 contributed to low level divergence and decreased rainfall over India in June. These results  
34 help to better understand the influence of the tropical SST anomalies on the seasonal evolution  
35 of ISM rainfall during extreme IOD events.

36

37 **Plain Language Summary**

38 A prominent pattern of variability in the Indian Ocean is a seesaw in sea surface temperature  
39 (SST) between the eastern and western sides of the Ocean basin, called the Indian Ocean Dipole  
40 (IOD). Its influence on the regional weather and climate is not yet fully established, but the  
41 extremely strong IOD event in 2019 provided us the opportunity to consider its impact on the  
42 Indian Summer Monsoon. By simulating the response to the anomalous SST patterns that  
43 occurred in 2019, and by observation-based analyses, we find evidence that the IOD did  
44 influence the monsoon rainfall in 2019, but that SST anomalies in the Pacific Ocean were also  
45 important. Our simulations show that the positive IOD was conducive to wetter-than-normal  
46 conditions throughout and especially at the end of the monsoon season, but that anomalous  
47 warmth in the central equatorial Pacific may have contributed to reduced rainfall in June over  
48 India. The results from this study help to understand the role of SST anomalies within and  
49 outside the Indian Ocean in affecting ISM rainfall intensity and seasonal evolution during  
50 extreme IOD events.

51

52

## 53 1 Introduction

54 The Indian Ocean Dipole (IOD) is one of the dominant modes of variability of the  
 55 tropical Indian Ocean which was discovered and named at the end of the 1990s (Saji et al 1999;  
 56 Webster et al 1999). The IOD has been recognized as being forced by ENSO (Allan et al.,  
 57 2001; Baquero-Bernal et al., 2002; Huang and Kinter, 2002; Dommenges, 2011; Zhao et al.,  
 58 2019) as well as a self-sustained mode of oscillation (Ashok et al., 2003; Yamagata et al., 2004;  
 59 Behera et al., 2006), with modelling frameworks supporting both hypotheses (Fischer et al.,  
 60 2005; Behera et al., 2006; Wang et al., 2019; Cretat et al., 2018). The IOD has also been  
 61 suggested as a potential trigger for ENSO (Luo et al., 2010; Izumo et al., 2010; Zhou et al.,  
 62 2015; Jourdain et al., 2016; Wieners et al., 2017; Wang et al., 2019; Cai et al., 2019), with IOD  
 63 events co-occurring with ENSO that may fasten its phase transition (Kug and Kang, 2006; Kug  
 64 and Ham, 2012). Past changes in the frequency and in the teleconnections of the IOD have  
 65 been documented on long time records (e.g. Abram et al., 2020).

66 The IOD teleconnections span from nearby countries like India (Ashok et al., 2001; Li  
 67 et al., 2003; Meehl et al., 2003; Wu and Kirtman, 2004; Cherchi et al., 2007; Krishnan et al.,  
 68 2011; Cherchi and Navarra, 2013; Krishnaswamy et al., 2015; Chowdary et al., 2016;  
 69 Srivastava et al., 2019, as some examples of the wide published literature available), Indonesia  
 70 (Pan et al., 2018), Africa (Black et al., 2003; Manatsa and Behera, 2013; Endris et al., 2019)  
 71 and Australia (i.e., [Cai et al., 2009](#); Ummenhofer et al., 2013; Dey et al., 2019; Hossain et al.,  
 72 2020), to more remote places, like Brazil (Chan et al., 2008; Taschetto and Ambrizzi, 2012;  
 73 Bazo et al., 2013).

74 Here we are particularly interested on the relationship between the IOD and the Indian  
 75 summer monsoon (ISM). Summer monsoon rainfall over India represents the largest source of  
 76 annual water for the country (Mall et al., 2006; Archer et al., 2010) and is important for the  
 77 agrarian economy (Gadgil and Gadgil, 2006; Webster et al., 1998). Despite its annual  
 78 occurrence, the Indian summer monsoon is highly variable in time and space, with the largest  
 79 portion of its variability modulated by ENSO, as known since the beginning of the 19th century  
 80 (Walker, 1924; Sikka, 1980; Rasmusson and Carpenter, 1983; Kirtman and Shukla, 2000;  
 81 Ratna et al 2011; Sikka and Ratna, 2011, as few examples). Toward the end of the 20<sup>th</sup> century  
 82 a weakening of the ISM-ENSO relationship has been identified (Kumar et al., 1999; Kinter et  
 83 al 2002) with the IOD recognized as a potential trigger of ISM rainfall. Several papers reported  
 84 the individual and combined influences of ENSO and IOD on ISM rainfall and found that both  
 85 phenomena, individually and combined, affect ISM rainfall performance (Ashok et al., 2004;  
 86 Sikka and Ratna, 2011; Krishnaswamy et al 2015; [Li et al., 2017](#); Hrudya et al 2020). Within

Deleted: ¶

The active and break spells of monsoons are regulated by the boreal summer intraseasonal oscillation (BSISO). As the BSISO propagates north from the equator into the Indian monsoon region its activity substantially affects the monsoon rainfall (Sikka and Gadgil 1980; Sperber et al., 2000).

Formatted: Highlight

the monsoon season, the mean structure of moisture convergence and meridional specific humidity distribution undergoes significant changes in contrasting IOD years, which in turn influences the meridional propagation of the boreal summer intra-seasonal oscillation (BSISO) and hence the related precipitation anomalies over India (Sikka and Gadgil, 1980; Sperber et al 2000; Ajayamohan et al., 2008). At this timescale, the ocean-atmosphere dynamical coupling has been found to be important to the extended Indian summer monsoon break of July 2002, for example (Krishnan et al 2006).

Some recent studies have investigated the causes of the strong IOD event in 2019. In particular, it has been found that The occurrence of 2019 extreme pIOD event features the strongest easterly and southerly wind anomalies on record, leading to the strongest wind speed that facilitated the latent cooling to overcome the increased radiative warming over the eastern equatorial Indian Ocean, leading to the unique thermodynamical forcing (Wang et al., 2020). The thermocline warming associated with anomalous ocean downwelling in the southwest tropical Indian Ocean triggered atmospheric convection to induce easterly winds anomaly along the equator and the positive feedbacks led to an IOD event (Du et al., 2020). Also, the record-breaking interhemispheric pressure gradient over the Indo-Pacific region induced northward cross-equatorial flow over the western Maritime Continent, able to trigger strong wind-evaporation-SST and thermocline feedbacks that contributed to the strong IOD (Lu and Ren, 2020). How the consecutive concurrence of the 2018 and 2019 positive Indian Ocean Dipole along with the evolution of a Central Pacific El Niño influenced the Australia climate is described in Wang and Cai (2020). The 2019 IOD event led to the unusual warm conditions in many parts of the East Asia during 2019–2020 winter (Doi et al 2020), even if this does not seem necessarily linked with the severe drought that occurred during that fall in East China (Ma et al 2020). In terms of predictability, such an extreme event like the 2019 IOD could be predicted a few seasons in advance (Doi et al., 2020).

In this study we intend to investigate the dynamical aspects of the relationship between IOD and Indian summer monsoon rainfall with a specific focus on 2019. That year was peculiar in terms of the seasonal evolution of precipitation over India with dry conditions at the beginning of the monsoon season and very wet conditions toward the end (Sunitha Devi et al., 2020). In particular, we designed a set of sensitivity experiments to verify the role of anomalous SST in the Indian Ocean, i.e. the developing IOD that year, and the SST anomalies elsewhere. The work is organized as follows: Section 2 describes the data used for the analysis as well as the model and experiments performed. Section 3 is dedicated to the observed characteristics of

Deleted: T

Deleted: Similarly, Krishnan et al. (2006) explored

Deleted: on intra-seasonal time-scales which was

Deleted:

Deleted: The above studies indicate the influential role of air–sea interaction on the genesis and propagation of BSISO and its impact on monsoon.

Deleted: f

Deleted: t

Deleted: In terms of the climate impact of this strong IOD event, Wang and Cai (2020) discussed

Deleted: h

Deleted:

Deleted: ing

Deleted: Doi et al (2020) found that

Deleted: t

IOD and ISM during 2019 with specific attention to the evolution within the summer season. Section 4 shows the results from the sensitivity experiments performed, including a discussion of the main results obtained. Finally, section 5 summarizes the main finding and provide future perspectives from this analysis.

## 2 Methods

### 2.1 Observed datasets and indices

The SST anomaly difference between the west (50°E-70°E, 10°S-10°N) and east (90°E-110°E, 10°S-0°) equatorial Indian Ocean, identified as the Dipole Mode Index (DMI; Saji et al., 1999), is used as the metric for the IOD and we computed it using three different datasets: Extended Reconstructed Sea Surface Temperature v5 (ERSST; Huang et al., 2017) available at 2° latitude-longitude degree resolution, National Oceanic and Atmospheric Administration optimum interpolation SST version 2 (NOAA OISSTv2; Reynolds et al., 2002) available at 0.25° resolution, and Hadley Centre Sea Ice and Sea Surface Temperature data set v1.1 (HadISST; Rayner et al., 2003) available at 1° resolution. Other indices used are: Nino3.4 (area averaged SST anomaly over equatorial Pacific, 5°N-5°S 170°W-120°W) from [https://psl.noaa.gov/gcos\\_wgsp/Timeseries/Nino34/](https://psl.noaa.gov/gcos_wgsp/Timeseries/Nino34/) and El Nino-Modoki (Ashok et al., 2007; Weng et al, 2007) from <http://www.jamstec.go.jp/virtualearth/general/en/index.html>.

For rainfall we used the Global Precipitation Climatology Project (GPCP) data (Adler et al., 2003) available at 2.5° resolution. Other atmospheric variables and the global SST field are taken from National Center for Environmental Prediction-Department of Energy (NCEP-DOE) Reanalysis 2 (Kanamitsu et al., 2002) available at 2.5degree resolution. All anomalies are calculated with respect to the 1981-2010 climatology.

### 2.2 The IGCM4 model and sensitivity experiments

The Intermediate General Circulation Model version 4 (IGCM4; Joshi et al. 2015) is a global spectral primitive equation atmospheric model with a spectral truncation at T42 (corresponding to 128x64 grid points in the horizontal) and 20 layers in the vertical, with the top at 50 hPa. This configuration, i.e. T42L20, is the standard for studies of the troposphere and climate (Joshi et al. 2015). IGCM4 has been extensively used in climate research, process modelling and atmospheric dynamics (van der Wiel et al., 2016; O' Callaghan et al., 2014; Ratna et al., 2020). The IGCM4 gives a good representation of the mean climate state (Joshi et al, 2015), in particular the simulated climatology and annual cycle over Asia is in reasonable

agreement with the reanalysis for temperature and precipitation (Ratna et al., 2020). The physical parameterization schemes used here are the same as in Joshi et al (2015) and Ratna et al (2020).

The set of experiments performed with the IGCM4 consist of a control simulation (CTRL) with prescribed SST obtained from a climatology (1981-2010) of the skin temperature in the NCEP-DOE Reanalysis 2 (Kanamitsu et al, 2002) and two sensitivity experiments where the 2019 SST anomaly is added to the CTRL climatology globally (IODglob) and only over the Indian Ocean (IODreg). All other boundaries conditions are the same as in CTRL. The surface albedo has been adjusted to indicate the presence or absence of sea ice according to whether the new surface temperature was below freezing. We used the greenhouse gas concentration in the model which is close to the 1995 value, the midpoint of the 1981-2010 climatology. For each simulation, the model is integrated for 55 years and the mean of the last 50 years is analysed, excluding the first five years as model spin up. These simulations are long enough to allow a clear separation of the response to the SST anomalies from the internally generated variability, especially for “noisy” variables such as precipitation.

### 3 2019 Indian Ocean Dipole and Indian Summer Monsoon

The Indian Ocean Dipole (IOD) was unusually strong in 2019 (Fig. 1a). The positive IOD event was the strongest of the last two decades, and possibly the strongest of the last 38 years. The Sep-Nov 2019 DMI was four standard deviations above the 1981-2010 climatology in the ERSST data. This exceeded the previous strong event of 1997 in the ERSST and NOAA-OI-SST datasets, while 1997 remained the strongest in HadISST (Fig. S1). The 2019 positive IOD phase arose from both negative SST anomalies over the eastern equatorial Indian Ocean (EEIO) and warm SST anomalies over the western equatorial Indian Ocean (WEIO) from June to October (Fig 1c-h). However, the evolution of the event was strongly determined by the EEIO, which largely cooled from climatological conditions in May to almost 1 K cooler than normal by October. On the other hand, the WEIO stayed more constant (i.e. less than 1 K warmer than normal) throughout the period (Fig. 1b).

The total seasonal (June-September) rainfall over India was 110% with respect to its long-term climatology (1871-2019), with the June rainfall quite low (67%) while the September ~~one~~ quite excessive (152%) (Sunitha Devi et al., 2020). These conditions have been part of large-scale rainfall anomalies observed in the regions surrounding the Indian Ocean in 2019 (Fig. 2a, d and g). In this study we are interested to understand what anomalous climate

Deleted: was

Deleted: it was

Deleted: r

conditions within the 2019 summer season contributed to monsoon rainfall variation from a dry June to a wet September over India.

The annual evolution of the IOD index is compared with ENSO associated indices for the year 2019 (Fig 1b). The IOD is strong compared to the rest of indices during 2019 so it is interesting to consider the role of IOD on the seasonal evolution of ISM rainfall. The IOD index intensified from July and reached its peak during October-November (Fig 1b), due to the strengthening of the SST anomaly in the EEIO, as noted above. Nino3.4 SST indicates that ENSO condition was slightly positive in June, before decreasing in strength to reach zero anomaly in September. El Nino Modoki index, which is indicator of a central Pacific SST anomaly, remained slightly above normal throughout the year (Fig. 1c-h).

Other three strong IOD events in the record (i.e. 1994, 1997, 2006) have been compared with 2019 in terms of the seasonal evolution and with respect to the equatorial central Pacific SST (Modoki index) and equatorial eastern Pacific SST (Fig. S2). In the year 1994, the positive IOD strengthened from June to August and contributed to excess ISM rainfall during this period. Although the central Pacific was warmer than normal (but with neutral El Nino condition, Fig S2) the IOD dominated contributing to larger than normal ISM rainfall (Ashok et al., 2004; Krishnan et al., 2010; Sikka and Ratna, 2011). During the year 1997, the positive IOD strengthened from June to September in concomitance to a strong El Nino that started developing from May. In 1997 when the ENSO co-occurred with the positive phase of the IOD, the ENSO-induced anomalous subsidence is neutralized/reduced by the anomalous IOD-induced convergence over the Bay of Bengal (Behera et al., 1999 and Ashok et al, 2001) and contributed to neutral ISM season (Table S1). During 2006, the onset of IOD was late compared to the other years considered (Fig. S2), as it started in July/August contributing to above normal ISM during July-September (Table S1). Again, although the eastern equatorial Pacific was warmer than normal the IOD contributed to this near excess rainfall season (Krishnan et al., 2010). Overall, out of these four years, the year 1994 and 2019 had excess ISM rainfall anomaly (i.e., 115% and 116% with respect to 1981-2010 climatology, Table S1). Instead, 1997 had normal ISM season (i.e. 102%) and 2006 just a bit larger (i.e 108%) (Table S1). During the monsoon season 1994 and 2019 IOD anomalies were stronger than 1997 and 2006 (Fig. S2), and this may be contributed to related strong ISM rainfall anomaly in the former years compared to the latter.

#### 4 Mechanisms contributing to the anomalous 2019 Indian summer monsoon rainfall

To understand the contribution that SST forcing may make to the 2019 rainfall variability over the Indian landmass, we compared the model simulated anomaly (IODglob and

Deleted: We can see that

Deleted: We also have compared the seasonal evolution of 2019 IOD event with

Deleted: o

Deleted: (1994, 1997, 2006)

Formatted: Indent: First line: 1,27 cm

Deleted: and analysed the ISM rainfall variation

Deleted: It is noted that out of these four years,

Moved down [1]: the year 1994 and 2019 had excess ISM with rainfall anomaly 115% and 116% respectively with respect to 1981-2010 climatology (Table S1). The year 1997 had normal (102%) ISM season whereas 2006 was near excess (108%) season. Although, the IOD events for the years

Deleted: 3

Deleted: ¶

Deleted: it was seen that

Deleted: was in its positive phase and had

Deleted: to

Deleted: e

Deleted: excess

Deleted: had

Deleted: at the time

Deleted: In case of

Deleted: event

Deleted: (

Deleted: 1994, 1997, 2019) which

Deleted: and this

Deleted: ed

Deleted: is

Moved (insertion) [1]

Deleted: with

Deleted: respectively

Deleted: (

Deleted: The year

Deleted: (102%)

Deleted: whereas

Deleted: was near excess (108%) season

Deleted: Although, the IOD events for the years 1997 and [1]

Deleted: d

Deleted: (June-September) the years

Deleted: was

Deleted: 6

Deleted: .

Deleted: T

Deleted: in 1994 and 2019

Deleted: 1997 and 2006

IODreg as explained in Section 2) with the observed anomaly. Following the design of the experiments, the comparison is focused in the identification of the rainfall pattern anomalies in the different cases. Of course, we do not expect perfect agreement, even were the model perfect, because of internal atmospheric variability unrelated to the 2019 SST anomalies. Nevertheless, both sensitivity experiments reproduce a dipole precipitation anomaly over the south equatorial Indian Ocean (dry in the east, wet in the west; Fig. 2a-c) during the whole monsoon season (June-September) that closely resembles the observed pattern. Observed Jun-Sep precipitation is above average over the Indian land mass and over the Bay of Bengal, and both experiments simulate a qualitatively similar pattern. Instead, the intensity of the anomaly is larger when the model is forced with only Indian Ocean SST anomalies (IODreg; Fig. 2c) compared to the global SST (IODglob) anomaly (Fig. 2b). This indicates the importance of the 2019 Indian Ocean SST anomaly in contributing to wet conditions over India, though it is modulated by SST anomalies elsewhere.

The comparison of the sensitivity experiments also illuminates on the possible mechanisms behind the two contrasting months of the season (i.e. dry June and wet September). In June, the model response to Indian Ocean SST forcing produces a stronger south-westerly monsoon flow and wet anomalies over western India (IODreg; Fig. 2f), whereas including SST anomalies from other ocean basins (IODglob; Fig. 2e) suppresses the wet anomaly and brings the simulated response closer to the observations (with the exception of the western Indian Ocean). The negative rainfall anomaly over EEIO is also stronger in IODglob compared to IODreg and more similar to the observations. On the other hand, both IODglob and IODreg experiments have a wet anomaly over India in September, as is also seen in the observations (though the observed anomaly is stronger and more extensive). These results indicate that the 2019 Indian Ocean SST anomalies suppress rainfall in the EEIO and favour a wetter than normal Indian monsoon, but that in June the latter is more than offset by a response to the SST anomaly outside the Indian Ocean, resulting in the dry anomaly, as it is observed.

Considering the whole 2019 season, stronger low-level southerly wind anomalies dominated over the Bay of Bengal due to low level divergence over EEIO associated with the very positive IOD (Fig. 2a,b,c). The low-level winds are similar to Behera and Ratnam (2018) where they show low level westerlies and southerlies towards India originated from the EEIO but they do not show any significant cross equatorial flow in their positive IOD events composite. Over the Arabian Sea, the IODreg simulation has stronger south-westerly anomaly compared to IODglob and hence simulates excess rainfall (Fig. 2a, b, c). In June, the dry



anomaly observed over India is related to low-level anomalous anticyclonic circulation over central-east India and adjacent Bay of Bengal and to anomalous easterlies prevailing in the peninsular India (Fig 2d). Both circulation features reduced the monsoon flow towards India and hence contributed to the negative rainfall anomaly over India. IODglob realistically simulated both these anomalous circulation features (Fig. 2e), whereas IODreg did not and it shows strong south-westerly flow reaching the Indian landmass (Fig. 2f). In September 2019, observations show that there was a strong **anomalous** south-westerly flow towards Indian landmass and associated cyclonic circulation over central west India, contributing to the excess rainfall (Fig. 2g). Both sensitivity experiments (Fig. 2h and 2i) simulated anomalously strong south-westerly flow and anomalous cyclonic circulation over India, though they are not as strong as observed.

~~Consistently with precipitation and low-level wind patterns, over the Maritime Continent and EEIO there is convergence in the upper troposphere~~ in September when the IOD is at its peak (Fig. 3b), ~~but such~~ convergence does not appear in June (Fig. 3a) when the IOD is developing and there are still warm SST anomalies over the equatorial Pacific (Fig. 1). In the IODglob experiment (Fig. 3c) we see that the model responds strongly to these equatorial Pacific SST anomalies in June, causing strong upper level divergence over east equatorial Pacific and convergence over the Maritime Continent. The opposite circulation is seen at lower levels (see Fig. S2 for the 850 hPa velocity potential and divergent winds) which causes low level divergence extending from the Maritime Continent to the Bay of Bengal and Indian landmass, contributing to negative rainfall anomaly in June. In IODreg, where the model is forced with the 2019 SST anomaly only over the Indian Ocean, the model responds with upper level (lower level) divergence (convergence) over the Indian Ocean and over India (extending from Australia via WEIO to India; Fig. 3e and S2), which would have contributed to a positive rainfall anomaly in June. The model simulated velocity potential anomaly explains the model simulated rainfall and its link with Indian Ocean and Pacific Ocean SST anomaly, and indicates that the response is more closely linked with the equatorial Pacific SST rather with the SST anomalies in the extratropical North Pacific which were also large in 2019. Both sensitivity experiments simulate upper level divergence over EEIO region in September, although in IODglob it is stronger than in IODreg, and this explains the link between the Indian Ocean SST anomaly and the circulation and rainfall anomalies.

Deleted: ed

Deleted: To understand how the Pacific Ocean and Indian Ocean together modulate the ISM rainfall we analyzed upper level velocity potential and divergent winds for the dry June and wet September months. There is upper level convergence o

Deleted: but such

## 376 5 Conclusions

377 One of the strongest positive IOD events in the historical period occurred in 2019. The  
 378 evolution of the 2019 IOD was characterized by a cold anomaly over the EEIO which started  
 379 strengthening from June and reached its peak in October, remaining strong until November. In  
 380 the same year, the Indian summer monsoon season experienced peculiar behaviour with weak  
 381 rainfall during June (despite the IOD index being already in its positive phase). Then the  
 382 monsoon gained its strength from July, ending with an anomalous wet September and  
 383 contributing to above-normal seasonal rainfall.

384 With a suite of atmospheric GCM experiments we have been able to evidence the role  
 385 of the IOD and of the SST anomalies elsewhere in the seasonal evolution of rainfall and  
 386 circulation anomalies during the 2019 summer monsoon. The anomalous SST gradient between  
 387 the west and east equatorial Indian Ocean drives a dipole in equatorial precipitation anomalies  
 388 and anomalous low-level circulation that would, in isolation, lead to a wetter than normal  
 389 Indian summer monsoon across the monsoon season including June and September. However,  
 390 when forcing the ICGM4 model with the global pattern of SST anomalies observed in 2019,  
 391 the response changes, particularly in June. Although not considered to be an El Nino, the first  
 392 half of 2019 did exhibit anomalously warm conditions in the central Pacific (visible in the  
 393 Nino3.4 index) that dissipated by September. The model responds to this equatorial Pacific  
 394 warmth with upper-level divergence over the equatorial Pacific and convergence over the  
 395 Maritime Continent. This causes low-level divergence extending from the Maritime Continent  
 396 to the Bay of Bengal and the Indian landmass, contributing to a negative rainfall anomaly there  
 397 in June. By September, this response to remote forcing from the Pacific weakens (likely linked  
 398 in part to the weakening of the Nino3.4 SST anomaly there), leaving the response to the Indian  
 399 Ocean SST anomalies (linked to the very strong IOD) to dominate. This response arises from  
 400 strong IOD-related low-level divergence over EEIO and convergence over the Indian  
 401 landmass, contributing to excessive rainfall.

402 The similarity between the model simulations and observed/reanalysis data provides  
 403 evidence that these mechanisms occurred in the real world in 2019, i.e. that there was a  
 404 contrasting contribution from the Pacific and Indian Ocean SST anomalies to ISM rainfall. The  
 405 tropical Pacific SST contributed to a drying tendency over India while the IOD contributed to  
 406 anomalous wet conditions over India. The Pacific effect dominated in June, contributing to the  
 407 dry anomalies observed, but the weakening Pacific SST anomalies and especially the dramatic  
 408 strengthening of the IOD led to the latter dominating by September and having a significant  
 409 contribution to the very wet September observed.

410 The observed June and September rainfall anomalies were more extreme than those  
 411 simulated in these SST-forced experiments, reinforcing the role that internal atmospheric  
 412 variability plays in any particular month or season. Nevertheless, the results from this study  
 413 help to understand the role of SST anomalies within and outside the Indian Ocean in affecting  
 414 ISM rainfall intensity and seasonal evolution during extreme IOD events. This is important for  
 415 improving seasonal predictions of Indian summer monsoon, and our results also highlight that,  
 416 to predict the seasonal evolution of ISM rainfall, Pacific SST anomalies must be considered  
 417 even when there is an extremely strong IOD. ~~For example, Li et al (2017) show that the~~  
 418 ~~majority of CMIP5 models simulate an unrealistic present-day IOD-ISM correlation due to~~  
 419 ~~an overly strong control by ENSO and hence a positive IOD is associated with the reduction~~  
 420 ~~of ISM rainfall in the simulated present-day climate. Hence, coupled climate models need to~~  
 421 ~~improve their simulation of these type of linkages.~~

Deleted: Also

Deleted: Thus, it is important that the

Deleted: that we found in this study

## 423 Acknowledgements

424 This study is supported by the Belmont Forum and JPI-Climate project INTEGRATE  
 425 (An Integrated data-model study of interactions between tropical monsoons and extratropical  
 426 climate variability and extremes) with funding by UK NERC grant NE/P006809/1. The model  
 427 experiments were conducted on the High Performance Compute Cluster at the University of  
 428 East Anglia. ~~We thank the two anonymous reviewers for their constructive comments.~~

## 430 Data Availability Statement

431 The data used in this study can be downloaded from the following websites:  
 432 ERSST (<https://psl.noaa.gov/data/gridded/data.noaa.ersst.v5.html>);  
 433 OISST (<https://psl.noaa.gov/data/gridded/data.noaa.oisst.v2.html>);  
 434 HadISST (<https://www.metoffice.gov.uk/hadobs/hadisst/>);  
 435 GPCP (<https://psl.noaa.gov/data/gridded/data.gpcp.html>);  
 436 NCEP-DOE Reanalysis 2 (<https://psl.noaa.gov/data/gridded/data.ncep.reanalysis2.html>)  
 437 Nino3.4 ([https://psl.noaa.gov/gcos\\_wgsp/Timeseries/Nino34/](https://psl.noaa.gov/gcos_wgsp/Timeseries/Nino34/));  
 438 El Niño Modoki (<http://www.jamstec.go.jp/virtualearth/general/en/index.html>);  
 439 ISM rainfall ([https://tropmet.res.in/static\\_pages.php?page\\_id=53](https://tropmet.res.in/static_pages.php?page_id=53))  
 440 The model used in this study is described in (Joshi et al. 2015;  
 441 <https://gmd.copernicus.org/articles/8/1157/2015/>)

Formatted: Italian

Field Code Changed

Formatted: Italian

Formatted: Italian



## References

- Abram, N. J., Wright, N. M., Ellis, B., Dixon, B. C., Wurtzel, J. B., England, M. H., et al. (2020). Coupling of Indo-Pacific climate variability over the last millennium. *Nature*, 579, 385-392. <https://doi.org/10.1038/s41586-020-2084-4>
- Adler, R. F., Huffman, G. J., Chang, A., Ferraro, R., Xie, P. P., Janowiak, J., et al. (2003). The version-2 global precipitation climatology project (GPCP) monthly precipitation analysis (1979-present). *Journal of Hydrometeorology*. [https://doi.org/10.1175/1525-7541\(2003\)004<1147:TVGPCP>2.0.CO;2](https://doi.org/10.1175/1525-7541(2003)004<1147:TVGPCP>2.0.CO;2)
- Allan, R. J., Chambers, D., Drosowsky, W., Hendon, H., Latif, M., Nicholls, N., et al. (2001). Is there an Indian Ocean dipole and is it independent of the El Niño-Southern Oscillation? *CLIVAR Exchanges*, 6, 18–22.
- Archer, D. R., Forsythe, N., Fowler, H. J., & Shah, S. M. (2010). Sustainability of water resources management in the Indus Basin under changing climatic and socio economic conditions. *Hydrology and Earth System Sciences*, 14(8):1669–80. <https://doi.org/10.5194/hess-14-1669-2010>
- Ashok, K., Guan, Z., & Yamagata, T. (2001). Impact of the Indian Ocean dipole on the relationship between the Indian monsoon rainfall and ENSO. *Geophysical Research Letters*, 28, 4499-4502. <https://doi.org/10.1029/2001GL013294>
- Ashok, K., Guan, Z., & Yamagata, T. (2003). A look at the relationship between the ENSO and the Indian Ocean Dipole. *Journal of the Meteorological Society of Japan*, 81, 41-56. <https://doi.org/10.2151/jmsj.81.41>
- Ashok, K., Guan, Z., Saji, N. H., & Yamagata, T. (2004). Individual and combined influences of ENSO and the Indian Ocean Dipole on the Indian summer monsoon. *Journal of Climate*. [https://doi.org/10.1175/1520-0442\(2004\)017<3141:IACIOE>2.0.CO;2](https://doi.org/10.1175/1520-0442(2004)017<3141:IACIOE>2.0.CO;2)
- Ashok, K., Behera, S. K., Rao, S. A., Weng, H., & Yamagata, T. (2007). El Niño Modoki and its possible teleconnection. *Journal of Geophysical Research: Oceans*, 112, C11007. <https://doi.org/10.1029/2006JC003798>
- Baquero-Bernal, A., Latif, M., & Legutke, S. (2002). On dipolelike variability of sea surface temperature in the tropical Indian Ocean. *Journal of Climate*, 15, 1358-1368. [https://doi.org/10.1175/1520-0442\(2002\)015<1358:ODVOSS>2.0.CO;2](https://doi.org/10.1175/1520-0442(2002)015<1358:ODVOSS>2.0.CO;2)
- Bazo, J., Lorenzo, M. D. L. N., & Porfirio Da Rocha, R. (2013). Relationship between monthly rainfall in NW peru and tropical sea surface temperature. *Advances in Meteorology*. <https://doi.org/10.1155/2013/152875>

- 481 Behera, S. K., & Ratnam, J. V. (2018). Quasi-asymmetric response of the Indian summer  
482 monsoon rainfall to opposite phases of the IOD. *Scientific Reports*.  
483 <https://doi.org/10.1038/s41598-017-18396-6>
- 484 Behera, S. K., Luo, J. J., Masson, S., Rao, S. A., Sakuma, H., & Yamagata, T. (2006). A CGCM  
485 study on the interaction between IOD and ENSO. *Journal of Climate*, 19, 1608-1705.  
486 <https://doi.org/10.1175/JCLI3797.1>
- 487 Black, E., Slingo, J., & Sperber, K. R. (2003). An observational study of the relationship  
488 between excessively strong short rains in coastal East Africa and Indian ocean SST. *Monthly*  
489 *Weather Review*, 31, 74-94. [https://doi.org/10.1175/1520-](https://doi.org/10.1175/1520-0493(2003)131<0074:AOSOTR>2.0.CO;2)  
490 [0493\(2003\)131<0074:AOSOTR>2.0.CO;2](https://doi.org/10.1175/1520-0493(2003)131<0074:AOSOTR>2.0.CO;2)
- 491 [Cai, W., Cowan, T., & Raupach, M. \(2009\). Positive Indian Ocean Dipole events precondition](#)  
492 [southeast Australia bushfires, \*Geophys. Res. Lett.\*, 36, L19710,](#)  
493 [doi: 10.1029/2009GL039902](#) Cai, W., Wu, L., Lengaigne, M., Li, T., McGregor, S., Kug, J.  
494 S., et al. (2019). Pantropical climate interactions. *Science*, 363, 6430.  
495 <https://doi.org/10.1126/science.aav4236>
- 496 Chan, S. C., Behera, S. K., & Yamagata, T. (2008). Indian Ocean Dipole influence on South  
497 American rainfall. *Geophysical Research Letters*, 35, L14S12.  
498 <https://doi.org/10.1029/2008GL034204>
- 499 Cherchi, A., & Navarra, A. (2013). Influence of ENSO and of the Indian Ocean Dipole on the  
500 Indian summer monsoon variability. *Climate Dynamics*, 41, 81-103.  
501 <https://doi.org/10.1007/s00382-012-1602-y>
- 502 Cherchi, A., Gualdi, S., Behera, S., Luo, J. J., Masson, S., Yamagata, T., & Navarra, A. (2007).  
503 The influence of tropical Indian Ocean SST on the Indian summer monsoon. In *Journal of*  
504 *Climate*, 20, 3083-3105. <https://doi.org/10.1175/JCLI4161.1>
- 505 Chowdary, J. S., Parekh, A., Kakatkar, R., Gnanaseelan, C., Srinivas, G., Singh, P., & Roxy,  
506 M. K. (2016). Tropical Indian Ocean response to the decay phase of El Niño in a coupled  
507 model and associated changes in south and east-Asian summer monsoon circulation and  
508 rainfall. *Climate Dynamics*, 47, 831-844. <https://doi.org/10.1007/s00382-015-2874-9>
- 509 Crétat, J., Terray, P., Masson, S., & Sooraj, K. P. (2018). Intrinsic precursors and timescale of  
510 the tropical Indian Ocean Dipole: insights from partially decoupled numerical experiment.  
511 *Climate Dynamics*, 51, 1311-1352. <https://doi.org/10.1007/s00382-017-3956-7>
- 512 Dey, R., Lewis, S. C., & Abram, N. J. (2019). Investigating observed northwest Australian  
513 rainfall trends in Coupled Model Intercomparison Project phase 5 detection and attribution

Deleted: ¶

Formatted: Italian

- 515 experiments. *International Journal of Climatology*, 39, 112-127.  
 516 <https://doi.org/10.1002/joc.5788>
- 517 Doi, T., Behera, S. K., & Yamagata, T. (2020). Predictability of the Super IOD Event in 2019  
 518 and Its Link With El Niño Modoki. *Geophysical Research Letters*, 47,  
 519 <https://doi.org/10.1029/2019GL086713>
- 520 Doi, T., Behera, S. K., & Yamagata, T. (2020). Wintertime impacts of the 2019 super IOD on  
 521 East Asia. *Geophysical Research Letters*, 47, e2020GL089456.  
 522 <https://doi.org/10.1029/2020GL089456>
- 523 Dommenges, D. (2011). An objective analysis of the observed spatial structure of the tropical  
 524 Indian Ocean SST variability. *Climate Dynamics*, 36, 2129-2145.  
 525 <https://doi.org/10.1007/s00382-010-0787-1>
- 526 Du, Y., Zhang, Y., Zhang, L.-Y., Tozuka, T., Ng, B., & Cai, W. (2020). Thermocline warming  
 527 induced extreme Indian Ocean dipole in 2019. *Geophysical Research Letters*, 47,  
 528 e2020GL090079. <https://doi.org/10.1029/2020GL090079>
- 529 Hewitson, B., Dosio, A., Nikulin, G., & Artan, G. A. (2019). Future changes in rainfall  
 530 associated with ENSO, IOD and changes in the mean state over Eastern Africa. *Climate*  
 531 *Dynamics*, 52, 2029-2053. <https://doi.org/10.1007/s00382-018-4239-7>
- 532 Fischer, A. S., Terray, P., Guilyardi, E., Gualdi, S., & Delecluse, P. (2005). Two independent  
 533 triggers for the Indian Ocean dipole/zonal mode in a coupled GCM. *Journal of Climate*,  
 534 18(17), 3428–3449. <https://doi.org/10.1175/JCLI3478.1>
- 535 Gadgil, S., & Gadgil, S. (2006). The Indian monsoon, GDP and agriculture. *Economic &*  
 536 *Political Weekly*, 41(47): 4887–4895.
- 537 Hossain, I., Rasel, H. M., Imteaz, M. A., & Mekanik, F. (2020). Long-term seasonal rainfall  
 538 forecasting using linear and non-linear modelling approaches: a case study for Western  
 539 Australia. *Meteorology and Atmospheric Physics*, 132, 131-141.  
 540 <https://doi.org/10.1007/s00703-019-00679-4>
- 541 Hrudya, P. H., Varikoden, H., & Vishnu, R. (2020). A review on the Indian summer monsoon  
 542 rainfall, variability and its association with ENSO and IOD. *Meteorology and Atmospheric*  
 543 *Physics*. <https://doi.org/10.1007/s00703-020-00734-5>
- 544 Huang, Bohua. (2002). Interannual variability in the tropical Indian Ocean. *Journal of*  
 545 *Geophysical Research*, 107 (C11). <https://doi.org/10.1029/2001jc001278>
- 546 Huang, Boyin, Thorne, P. W., Banzon, V. F., Boyer, T., Chepurin, G., Lawrimore, J. H., et al.  
 547 (2017). Extended reconstructed Sea surface temperature, Version 5 (ERSSTv5): Upgrades,

Formatted: Italian

Deleted: ¶

Formatted: Italian

- 549 validations, and intercomparisons. *Journal of Climate*. [https://doi.org/10.1175/JCLI-D-16-](https://doi.org/10.1175/JCLI-D-16-0836.1)
- 550 0836.1
- 551 Sunitha Devi, S., Mishra, K., Singh, S. P., Kumar, N., Kashyapi, A. & K. Sathi Devi (2020).
- 552 Regional characteristics of the 2019 southwest monsoon, Monsoon 2019 – A Report. IMD
- 553 Met Monograph.
- 554 [http://imdpune.gov.in/Clim\\_Pred\\_LRF\\_New/Reports/Monsoon\\_Report\\_2019/Chapter\\_1](http://imdpune.gov.in/Clim_Pred_LRF_New/Reports/Monsoon_Report_2019/Chapter_1.pdf)
- 555 [.pdf](http://imdpune.gov.in/Clim_Pred_LRF_New/Reports/Monsoon_Report_2019/Chapter_1.pdf)
- 556 Izumo, T., Vialard, J., Lengaigne, M., De Boyer Montegut, C., Behera, S. K., Luo, J. J., et al.
- 557 (2010). Influence of the state of the Indian Ocean Dipole on the following years El Niño.
- 558 *Nature Geoscience*, 3, 168-172. <https://doi.org/10.1038/ngeo760>
- 559 Joshi, M., Stringer, M., Van Der Wiel, K., O’Callaghan, A., & Fueglistaler, S. (2015). IGCM4:
- 560 A fast, parallel and flexible intermediate climate model. *Geoscientific Model Development*.
- 561 <https://doi.org/10.5194/gmd-8-1157-2015>
- 562 Jourdain, N. C., Lengaigne, M., Vialard, J., Izumo, T., & Gupta, A. Sen. (2016). Further
- 563 insights on the influence of the Indian Ocean dipole on the following year’s ENSO from
- 564 observations and CMIP5 models. *Journal of Climate*, 29, 637-658.
- 565 <https://doi.org/10.1175/JCLI-D-15-0481.1>
- 566 Kanamitsu, M., Ebisuzaki, W., Woollen, J., Yang, S. K., Hnilo, J. J., Fiorino, M., & Potter, G.
- 567 L. (2002). NCEP-DOE AMIP-II reanalysis (R-2). *Bulletin of the American Meteorological*
- 568 *Society*, 83, 1631–1643. <https://doi.org/10.1175/bams-83-11-1631>
- 569 Kinter, I. L., Miyakoda, K., & Yang, S. (2002). Recent change in the connection from the Asian
- 570 monsoon to ENSO. *Journal of Climate*, 15, 1203-1215. [https://doi.org/10.1175/1520-](https://doi.org/10.1175/1520-0442(2002)015<1203:RCITCF>2.0.CO;2)
- 571 0442(2002)015<1203:RCITCF>2.0.CO;2
- 572 Kirtman, B. P., & Shukla, J. (2000). Influence of the Indian summer monsoon on ENSO.
- 573 *Quarterly Journal of the Royal Meteorological Society*, 126, 213-239.
- 574 <https://doi.org/10.1002/qj.49712656211>
- 575 Krishnan, R., Ayantika, D. C., Kumar, V., & Pokhrel, S. (2011). The long-lived monsoon
- 576 depressions of 2006 and their linkage with the Indian Ocean Dipole. *International Journal*
- 577 *of Climatology*, 31, 1334-1352. <https://doi.org/10.1002/joc.2156>
- 578 Krishnaswamy, J., Vaidyanathan, S., Rajagopalan, B., Bonell, M., Sankaran, M., Bhalla, R. S.,
- 579 & Badiger, S. (2015). Non-stationary and non-linear influence of ENSO and Indian Ocean
- 580 Dipole on the variability of Indian monsoon rainfall and extreme rain events. *Climate*
- 581 *Dynamics*, 45, 175-184. <https://doi.org/10.1007/s00382-014-2288-0>



- 582 Kug, J. S., & Ham, Y. G. (2012). Indian ocean feedback to the ENSO transition in a multimodel  
583 ensemble. *Journal of Climate*, 25, 6942-6957. <https://doi.org/10.1175/JCLI-D-12-00078.1>
- 584 Kug, J. S., Kirtman, B. P., & Kang, I. S. (2006). Interactive feedback between ENSO and the  
585 Indian Ocean in an interactive ensemble coupled model. *Journal of Climate*, 19, 1784-1801.  
586 <https://doi.org/10.1175/JCLI3980.1>
- 587 Kumar, K. K., Rajagopalan, B., & Cane, M. A. (1999). On the weakening relationship between  
588 the indian monsoon and ENSO. *Science*, 284, 2156-2159.  
589 <https://doi.org/10.1126/science.284.5423.2156>
- 590 Li, T., Wang, B., Chang, C. P., & Zhang, Y. (2003). A theory for the Indian Ocean dipole-  
591 zonal mode. *Journal of the Atmospheric Sciences*, 60, 2119-2135.  
592 [https://doi.org/10.1175/1520-0469\(2003\)060<2119:ATFTIO>2.0.CO;2](https://doi.org/10.1175/1520-0469(2003)060<2119:ATFTIO>2.0.CO;2)
- 593 [Li, Z., Lin, X. & Cai, W. \(2017\). Realism of modelled Indian summer monsoon correlation](#)  
594 [with the tropical Indo-Pacific affects projected monsoon changes. \*Scientific Reports\*, 7,](#)  
595 [4929. <https://doi.org/10.1038/s41598-017-05225-z>](#)
- 596 Lu, B., & Ren, H. L. (2020). What Caused the Extreme Indian Ocean Dipole Event in 2019?  
597 *Geophysical Research Letters*, 47, e2020GL087768. <https://doi.org/10.1029/2020GL087768>
- 598 Luo, J. J., Zhang, R., Behera, S. K., Masumoto, Y., Jin, F. F., Lukas, R., & Yamagata, T.  
599 (2010). Interaction between El Niño and extreme Indian Ocean dipole. *Journal of Climate*,  
600 23, 726-742. <https://doi.org/10.1175/2009JCLI3104.1>
- 601 [Ma, S. M., C. W. Zhu, and J. Liu, 2020: Combined impacts of warm central equatorial Pacific](#)  
602 [sea surface temperatures and anthropogenic warming on the 2019 severe drought in East](#)  
603 [China. \*Adv. Atmos. Sci.\*, 37\(11\), 1149–1163, <https://doi.org/10.1007/s00376-020-0077-8>.](#)
- 604 Mall, R. K., Gupta, A., Singh, R., Singh, R. S., & Rathore, L. S. (2006). Water resources and  
605 climate change: An Indian perspective. *Current Science*, 90(12):1610–26.
- 606 [Manatsa, D., & Behera, S. K. \(2013\). On the epochal strengthening in the relationship between](#)  
607 [rainfall of East Africa and IOD. \*Journal of Climate\*, 26, 5655-5673.](#)  
608 <https://doi.org/10.1175/JCLI-D-12-00568.1>
- 609 Meehl, G. A., Arblaster, J. M., & Loschnigg, J. (2003). Coupled ocean-atmosphere dynamical  
610 processes in the tropical Indian and Pacific Oceans and the TBO. *Journal of Climate*, 16,  
611 2138-2158. <https://doi.org/10.1175/2767.1>
- 612 O'Callaghan, A., Joshi, M., Stevens, D., & Mitchell, D. (2014). The effects of different sudden  
613 stratospheric warming types on the ocean. *Geophysical Research Letters*.  
614 <https://doi.org/10.1002/2014GL062179>

Formatted: Italian

Formatted: English (US)

Formatted: English (US)

Formatted: English (US)

Field Code Changed

Formatted: Italian

- 615 Pan, X., Chin, M., Ichoku, C. M., & Field, R. D. (2018). Connecting Indonesian Fires and  
 616 Drought With the Type of El Niño and Phase of the Indian Ocean Dipole During 1979–  
 617 2016. *Journal of Geophysical Research: Atmospheres*, 123, 7974–7988.  
 618 <https://doi.org/10.1029/2018JD028402>
- 619 Rasmusson, E. M., & Carpenter, T. H. (1983). The relationship between eastern equatorial  
 620 Pacific sea surface temperatures and rainfall over India and Sri Lanka. *Monthly Weather*  
 621 *Review*, 111, 517–528. [https://doi.org/10.1175/1520-](https://doi.org/10.1175/1520-0493(1983)111<0517:TRBEEP>2.0.CO;2)  
 622 [0493\(1983\)111<0517:TRBEEP>2.0.CO;2](https://doi.org/10.1175/1520-0493(1983)111<0517:TRBEEP>2.0.CO;2)
- 623 Ratna, Satyaban B., Osborn, T. J., Joshi, M., & Luterbacher, J. (2020). The influence of atlantic  
 624 variability on asian summer climate is sensitive to the pattern of the sea surface temperature  
 625 anomaly. *Journal of Climate*, 33, 7567–7590. <https://doi.org/10.1175/JCLI-D-20-0039.1>
- 626 Ratna, Satyaban Bishoyi, Sikka, D. R., Dalvi, M., & Venkata Ratnam, J. (2011). Dynamical  
 627 simulation of Indian summer monsoon circulation, rainfall and its interannual variability  
 628 using a high resolution atmospheric general circulation model. *International Journal of*  
 629 *Climatology*, 31, 1927–1942. <https://doi.org/10.1002/joc.2202>
- 630 Rayner, N. A., Parker, D. E., Horton, E. B., Folland, C. K., Alexander, L. V., Rowell, D. P., et  
 631 al. (2003). Global analyses of sea surface temperature, sea ice, and night marine air  
 632 temperature since the late nineteenth century. *Journal of Geophysical Research:*  
 633 *Atmospheres*. <https://doi.org/10.1029/2002jd002670>
- 634 Reynolds, R. W., Smith, T. M., Liu, C., Chelton, D. B., Casey, K. S., & Schlax, M. G. (2007).  
 635 Daily high-resolution-blended analyses for sea surface temperature. *Journal of Climate*.  
 636 <https://doi.org/10.1175/2007JCLI1824.1>
- 637 Saji, N. H., Goswami, B. N., Vinayachandran, P. N., & Yamagata, T. (1999). A dipole mode  
 638 in the tropical Indian ocean. *Nature*, 401, 360–363. <https://doi.org/10.1038/43854>
- 639 Sikka, D. R. (1980). Some aspects of the large scale fluctuations of summer monsoon rainfall  
 640 over India in relation to fluctuations in the planetary and regional scale circulation  
 641 parameters. *Proceedings of the Indian Academy of Sciences - Earth and Planetary Sciences*,  
 642 89, 179–195. <https://doi.org/10.1007/BF02913749>
- 643 Sikka, D. R., & Ratna, S. B. (2011). On improving the ability of a high-resolution atmospheric  
 644 general circulation model for dynamical seasonal prediction of the extreme seasons of the  
 645 Indian summer monsoon. *Mausam*, 62 (3), 339–360.
- 646 Srivastava, A., Pradhan, M., Goswami, B. N., & Rao, S. A. (2019). Regime shift of Indian  
 647 summer monsoon rainfall to a persistent arid state: external forcing versus internal

Formatted: Italian

Formatted: Italian

Formatted: Italian

- variability. *Meteorology and Atmospheric Physics*, 131, 211-224.  
<https://doi.org/10.1007/s00703-017-0565-2>
- Taschetto, A. S., & Ambrizzi, T. (2012). Can Indian Ocean SST anomalies influence South American rainfall? *Climate Dynamics*, 38, 1615-1628. <https://doi.org/10.1007/s00382-011-1165-3>
- Ummenhofer, C. C., Schwarzkopf, F. U., Meyers, G., Behrens, E., Biastoch, A., & Böning, C. W. (2013). Pacific ocean contribution to the asymmetry in eastern indian ocean variability. *Journal of Climate*, 26, 1152-1171. <https://doi.org/10.1175/JCLI-D-11-00673.1>
- Walker, G. T. (1924). Correlation in seasonal variations of weather - A further study of world weather. *Mon. Wea. Rev.*, 53, 252-254, [https://doi.org/10.1175/1520-0493\(1925\)53<252:CISVOW>2.0.CO;2](https://doi.org/10.1175/1520-0493(1925)53<252:CISVOW>2.0.CO;2).
- Wang, G., Cai, W., Yang, K., Santoso, A., & Yamagata, T. (2020). A Unique Feature of the 2019 Extreme Positive Indian Ocean Dipole Event. *Geophysical Research Letters*, 47, e2020GL088615. <https://doi.org/10.1029/2020GL088615>
- Wang, G., Cai, W. (2020) Two-year consecutive concurrences of positive Indian Ocean Dipole and Central Pacific El Nino preconditioned the 2019/2020 Australian "black summer" bushfires. *Geosci. Lett.* 7, 19. <https://doi.org/10.1186/s40562-020-00168-2>
- Wang, H., Kumar, A., Murtugudde, R., Narapusetty, B., & Seip, K. L. (2019). Covariations between the Indian Ocean dipole and ENSO: a modeling study. *Climate Dynamics*, 53, 5743-5761. <https://doi.org/10.1007/s00382-019-04895-x>
- Webster, P. J., Magaña, V. O., Palmer, T. N., Shukla, J., Tomas, R. A., Yanai, M., & Yasunari, T. (1998). Monsoons: processes, predictability, and the prospects for prediction. *Journal of Geophysical Research: Oceans*, 103(C7):. <https://doi.org/10.1029/97jc02719>
- Webster, Peter J., Moore, A. M., Loschnigg, J. P., & Leben, R. R. (1999). Coupled ocean-atmosphere dynamics in the Indian Ocean during 1997-98. *Nature*, 401, 356-360. <https://doi.org/10.1038/43848>
- Weng, H., Ashok, K., Behera, S. K., Rao, S. A., & Yamagata, T. (2007). Impacts of recent El Niño Modoki on dry/wet conditions in the Pacific rim during boreal summer. *Climate Dynamics*, 29(2-3), 113-129. <https://doi.org/10.1007/s00382-007-0234-0>
- van der Wiel, K., Matthews, A. J., Joshi, M. M., & Stevens, D. P. (2016). The influence of diabatic heating in the South Pacific Convergence Zone on Rossby wave propagation and the mean flow. *Quarterly Journal of the Royal Meteorological Society*. <https://doi.org/10.1002/qj.2692>

681 Wieners, C. E., Dijkstra, H. A., & de Ruijter, W. P. M. (2017). The influence of the Indian  
682 Ocean on ENSO stability and flavor. *Journal of Climate*, 30, 2601-2620.  
683 <https://doi.org/10.1175/JCLI-D-16-0516.1>

684 Wu, R., & Kirtman, B. P. (2004). Impacts of the Indian Ocean on the Indian Summer Monsoon-  
685 ENSO relationship. *Journal of Climate*, 17, 3037-3054. [https://doi.org/10.1175/1520-0442\(2004\)017<3037:IOTIOO>2.0.CO;2](https://doi.org/10.1175/1520-0442(2004)017<3037:IOTIOO>2.0.CO;2)

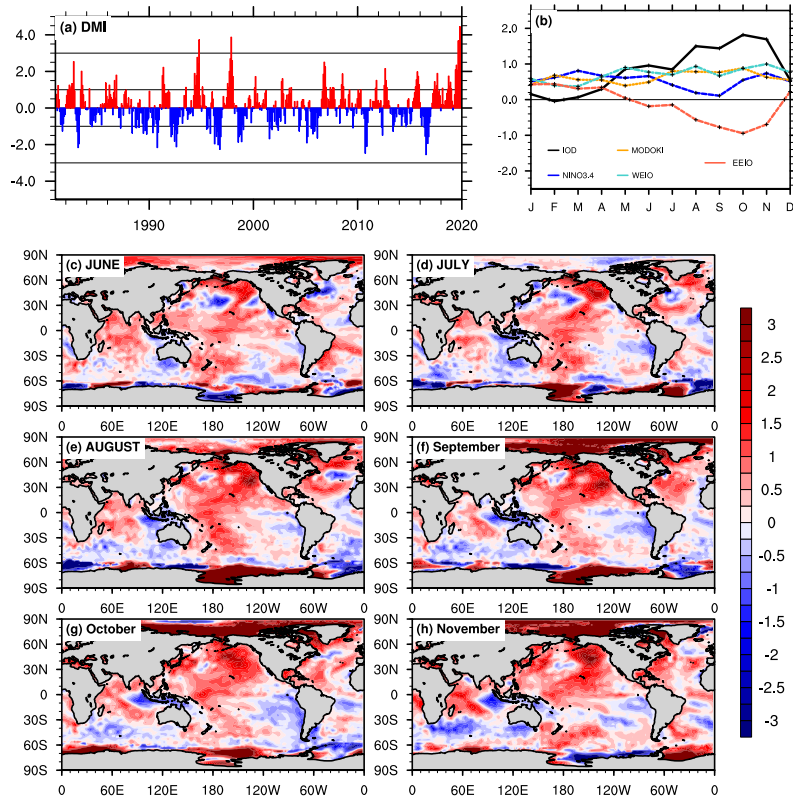
686  
687 Yamagata, T., Behera, S. K., Luo, J. J., Masson, S., Jury, M. R., & Rao, S. A. (2004). Coupled  
688 ocean-atmosphere variability in the tropical Indian ocean. *Geophysical Monograph Series*,  
689 147, 189–211. <https://doi.org/10.1029/147GM12>

690 Zhao, S., Jin, F. F., & Stuecker, M. F. (2019). Improved Predictability of the Indian Ocean  
691 Dipole Using Seasonally Modulated ENSO Forcing Forecasts. *Geophysical Research*  
692 *Letters*, 46, 9980-9990. <https://doi.org/10.1029/2019GL084196>

693 Zhou, Q., Duan, W., Mu, M., & Feng, R. (2015). Influence of positive and negative Indian  
694 Ocean Dipoles on ENSO via the Indonesian Throughflow: Results from sensitivity  
695 experiments. *Advances in Atmospheric Sciences*, 32, 783-793.  
696 <https://doi.org/10.1007/s00376-014-4141-0>

697  
698  
699  
700  
701  
702  
703  
704

705 **Figures:**



706  
707  
708 Fig. 1: (a) Standardized monthly Dipole Mode Index (DMI) from 1980 to 2019 calculated using  
709 ERSST data. (b) Annual cycle of Indian and Pacific Oceans climate indices (K) for 2019 (as  
710 discussed in Section 2). (c-h) Observed 2019 SST anomalies from June to November using  
711 NCEP2 data.

712

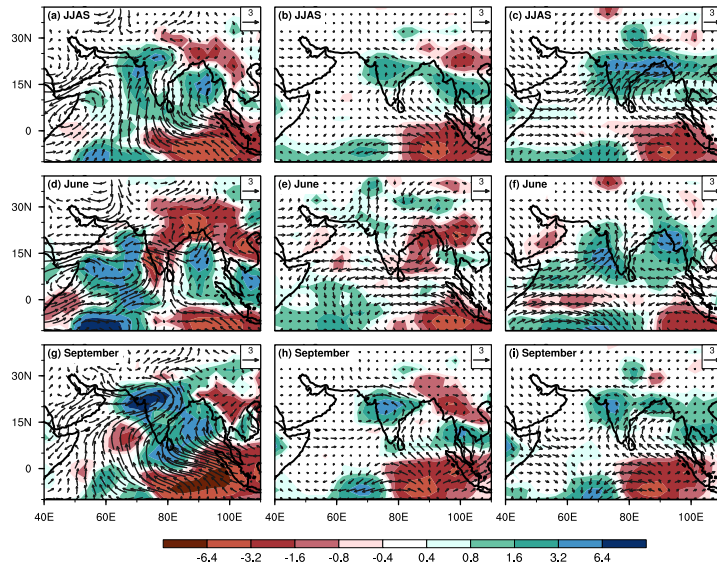


Fig. 2: (a, d, g) Observed GPCP rainfall anomaly (mm/day, shaded) and NCEP2 850 hPa wind anomaly (m/s, vectors) for June-September mean, June and September, respectively. (b,e,h) and (c,f,i) are the same as (a,d,g) but for IODglob and IODreg experiments, respectively. Shaded precipitation anomalies are significant at 90% level using a Student's t-test.

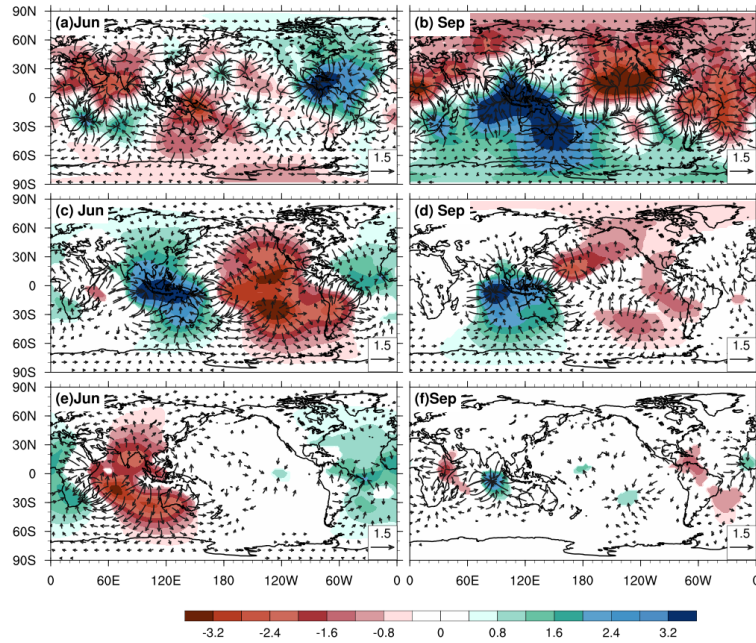


Fig. 3: (a,b) 200 hPa velocity potential ( $10^6 \text{ m}^2 \text{ s}^{-1}$ , shaded) and divergent wind ( $\text{m s}^{-1}$ , vectors) anomalies in 2019 June and September, respectively, based on the reanalysis. (c, d) and (e,f) are the same as (a,b) but for IODglob and IODreg experiments, respectively. Shaded velocity potential anomalies are significant at 90% level using a Student's t-test.

▼ ..... ◀

▲ .....